Distribution of relaxation times in α-phase polyvinylidene fluoride

Enis Tuncer *, Michael Wegener, Reimund Gerhard-Multhaupt

Applied Condensed-Matter Physics, Department of Physics, University of Potsdam, D-14469 Potsdam, Germany

Abstract

In this paper, a recently developed numerical method to analyze dielectric-spectroscopy data is applied to α-phase polyvinylidene fluoride (PVDF). The numerical procedure is non-parametric and does not contain any of the extensively used empirical formulas mentioned in the literature. The method basically recovers the unknown distribution of relaxation times of the generalized dielectric function representation by simultaneous application of the Monte Carlo integration method and of the constrained least-squares optimization. The relaxation map constructed after the numerical analysis is compared to α-phase PVDF data presented in the literature and results of the parametric analysis with a well-known empirical formula.

Key words: Dielectric spectroscopy, distribution of relaxation times, Monte Carlo integration, constrained least-squares.

Dielectric spectroscopy is a well established tool for materials characterization [1]. With this technique, the complex dielectric permittivity $\varepsilon(\omega)$ is obtained as a function of angular frequency ω ($\omega = 2\pi\nu$; ν is the frequency of the applied voltage). Analysis of $\varepsilon(\omega)$ is usually performed with empirical formulas [2, 3, 4, 5]. A neglected approach is the distribution of relaxation times (DRT), which is based on functional analysis (it requires the solution of an integral equation) [6]. The DRT expression is a Volterra equation [7], which is a special form of the Fredholm integral equations [8]. Such equations are usually considered to be *ill-conditioned* because of their non-unique solutions. However, the approach used here and recently presented elsewhere [5, 9, 10, 11] leads to unique solutions by means of a constrained least-squares fit and the Monte Carlo integration method. Macdonald [12] stated that approaches with summations of delta functions would not suffer from the limitations of ill-posed

* Corresponding author.
Email address: enis.tuncer@physics.org (Enis Tuncer).

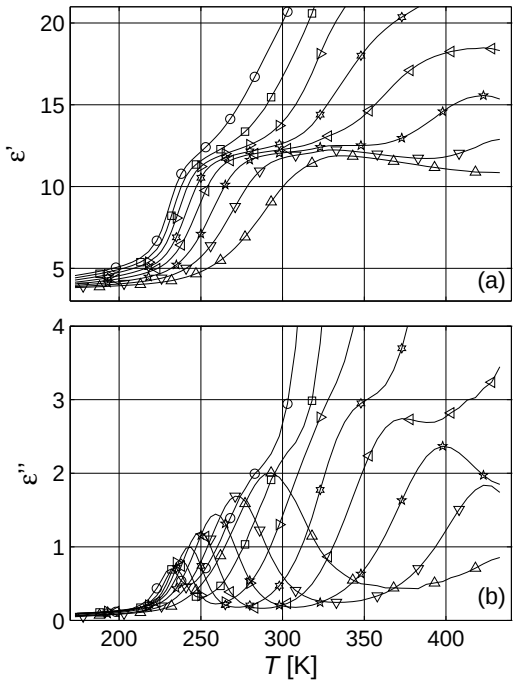

Fig. 1. (a) Real and (b) imaginary parts of α-phase PVDF dielectric function of temperature at various frequencies ν: ($\circ$) 0.1 Hz, ($\square$) 1 Hz, ($\triangleright$) 10 Hz, ($\hexagram$) 100 Hz, ($\triangleleft$) 1 kHz, ($\star$) 10 kHz, ($\bigtriangledown$) 100 kHz and ($\bigtriangleup$) 1 MHz. The lines are drawn to guide the eyes.

inversions if complex nonlinear least-squares are employed, another approach to solve inverse problems. In this paper, we apply this numerical procedure that was developed by one of us (ET) to a semi-crystalline polymer, α-phase polyvinylidene fluoride (α-phase PVDF) [13, 14, 15, 16]. An empirical formula and results from the literature are also included in order to evaluate the new DRT approach and to compare several analyzing techniques. Impedance measurements on α-phase PVDF are performed at various tempatures T between 173 K and 450 K within frequency windows of 0.1 Hz $\leq \nu \leq$ 1 MHz.

In Fig. 1, the relaxation spectra of α-phase PVDF are shown at several frequencies as a function of temperature. Local movements of the structural units in α-phase PVDF are observed at low temperatures, $T \lesssim 250$ K. This relaxation is usually called β relaxation. In α-phase PVDF, the magnitude of the β-relaxation is much smaller than those of two α-relaxations. The α-relaxations are related to cooperative movements of segments of the macromolecular chains. The subscripts 'a' and 'c' denote the fast asymmetric (amorphous) and the slow symmetric (crystalline) relaxation modes in the material [13, 14], respectively.

The dielectric function of a material can be expressed in a general forma as follows,

$$\varepsilon(\omega) = \epsilon + \chi(\omega) + \sigma/(\imath\varepsilon_0\omega), \tag{1}$$

where ϵ and σ are the frequency-independent relative dielectric permittivity and the ohmic conductivity of the material, $\imath = \sqrt{-1}$ and $\varepsilon_0 = 8.854$ pFm^{-1}.

$\chi(\omega)$ is the susceptibility of the material which is usually expressed through the Havriliak-Negami empirical formula (HNEF) [17] as

$$\chi(\omega) = \sum_j \Delta\varepsilon_j [1 + (\imath\omega\tau_j)^{\alpha_j}]^{-\beta_j}. \tag{2}$$

Here, we consider that there are several relaxation processes in the material (summation over j). The parameters τ_j and $\Delta\varepsilon_j$ are the most probable relaxation time and the magnitude of the related polarization relaxation, respectively. The parameters α_j and β_j determine the shape of the relaxation, $\alpha_j \leq 1$ and $\alpha_j\beta_j \leq 1$ [18]. A curve-fitting procedure based on the complex-nonlinear-least-squares (CNLSQ) method would yield the four unknowns for each relaxation $\{\tau, \Delta\varepsilon, \alpha, \beta\}$, as well as the high-frequency dielectric permittivity ϵ and the ohmic losses proportional to σ [3, 4].

In the DRT representation, the susceptibility $\chi(\omega)$ of Eq. (1) is expressed as

$$\chi(\omega) = \Delta\varepsilon \int_0^\infty \mathsf{g}(\tau)(1 + \imath\omega\tau)^{-1} \mathrm{d}\tau, \tag{3}$$

where $\mathsf{g}(\tau)$ is the distribution of relaxation times. Eq. (3) is the Volterra equation [7] and $(1 + \imath\omega\tau)^{-1}$ its *kernel* $\mathcal{K}(\omega, \tau)$. For the numerical procedure, several relaxation times τ_k are selected from a log-linear scale on the frequency axis [5, 9]. The number k of the relaxations is smaller than the total number n of experimental data points. In that case, the integral equation in Eq. (3) becomes a sum that is linear in the g_k,

$$\chi(\omega) = \Delta\varepsilon \sum_k \mathsf{g}_k \; \mathcal{K}(\omega, \tau_k) \tag{4}$$

Since the g_k are expected to be positive, $\mathsf{g}_k \geq 0$, a constrained least-squares algorithm is employed [19, 20] with newly selected τ sets for N times. α-phase PVDF had previously been analyzed by Grimau et al. [14] and by Bella et al. [13]. They used a Metropolis algorithm to obtain the relaxation characteristics of α-phase PVDF.

Below, we first present and compare the results obtained from HNEF and DRT analyses at 173 K. In Fig. 2, HNEF analysis is plotted. The symbols in Fig. 2a are the experimental values, and the line is the curve fitted with Eq. (2) for $j = 2$. The relative error δ of the real and imaginary parts of $\varepsilon(\omega)$ are presented in Fig. 2b. We illustrate the relative error in order to compare the DRT analysis with other methods. The average magnitude of the error in the imaginary part $\delta\varepsilon''$ is approximately ten times higher than that of the real part $\delta\varepsilon'$, $\delta\varepsilon'' \simeq 10\ \delta\varepsilon'$. In addition, a detailed analysis of the data shows that 90%

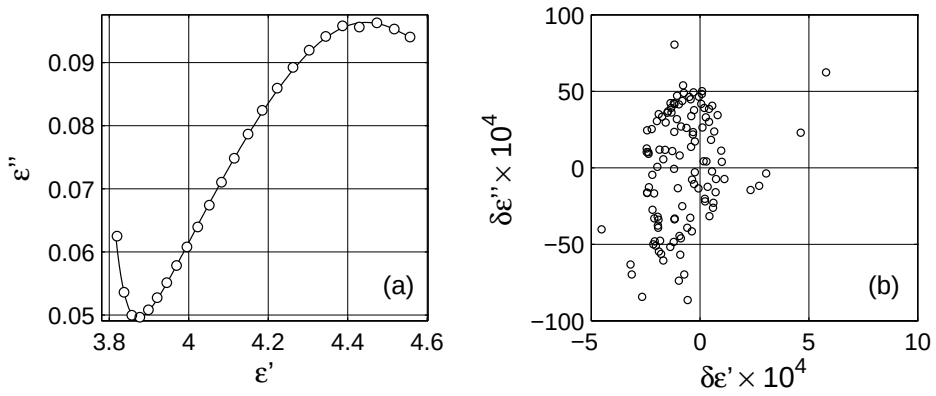

Fig. 2. (a) Cole-Cole parametric plot of the dielectric function at 173 K. The symbols and the line represent the experimental data and the curve obtained from CNLSQ with the Havriliak-Negami empirical formula, respectively. (b) Relative error δ of the CNLSQ fitting.

and 80% of the data fall into the region $\delta\varepsilon'' < 58 \times 10^{-4}$ and $\delta\varepsilon'' < 48 \times 10^{-4}$, respectively.

In Fig. 3, the DRT analysis based on Eq. (3) is presented. Here, the data are divided into three regions (the results are presented in Fig. 3a and 3b with open symbols). The number of relaxation times in each minimization step is chosen to be 2/3 of the number of the experimental data points. The Monte Carlo loop N, which is the number of minimizations performed, is 2^{12}. The average magnitude of the error in ε'' is again approximately ten times that of the real part, $\delta\varepsilon'' \simeq 10\delta\varepsilon'$, as shown in Fig. 3b. Compared to the HNEF, the DRT analysis yields lower relative errors. 90% and 80% of all the data points fall into the region $\delta\varepsilon'' < 40 \times 10^{-4}$ and $\delta\varepsilon'' < 26 \times 10^{-4}$, respectively. These values are nearly 50% lower than the corresponding values of the HNEF analysis. In addition, the distribution of the errors is more symmetric than with the HNEF analysis. The extracted DRT spectrum is presented in Fig. 3c, which is plotted with error bars after presenting the data in bins. The numerical procedure predicts smooth continuations of the relaxation times τ outside the experimental window. The experimental frequency window is indicated with dashed vertical lines (- - -) in Fig. 3c.

Application of the DRT analysis to data at different temperatures yields distributions similar to that presented in Fig. 3c. Lévy statistics [21, 22] will be later used to assess these distributions (see Refs. [10, 11]). The mean relaxation times from the Lévy statistics and from the HNEF analysis are employed to calculate the temperature dependence of the relaxations with the Vogel-Fulcher-Tammann (VFT) expression [23, 24, 25],

$$\tau = \tau_0 \exp\{W[k_b(T + T_0)]^{-1}\} \tag{5}$$

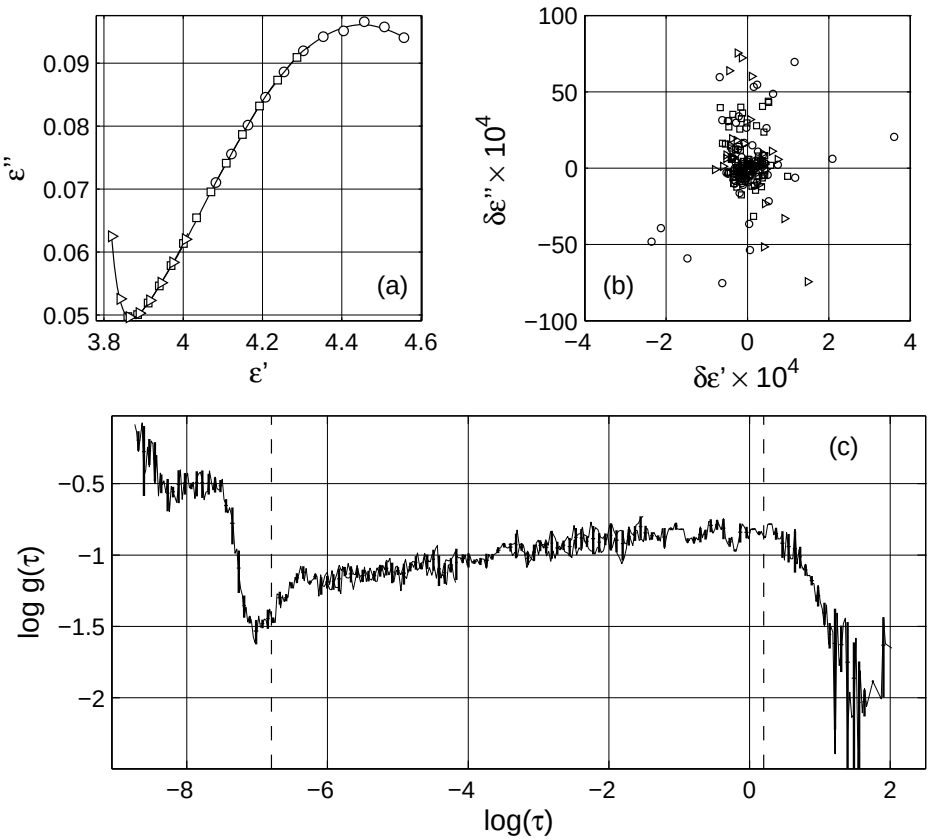

Fig. 3. (a) Cole-Cole parametric plot of the dielectric function at 173 K, the symbols and the line represent the experimental data and the curve obtained from the DRT analysis, respectively. The frequency window is divided into three regions on the frequency-axis, which are indicated with different symbols ('∘';high, '□';intermediate and '▷';low). (b) Relative error δ of the DRT analysis. (c) The DRT of α-phase PVDF for the experimental window 0.1 Hz $\leq \nu \leq$ 1 MHz; the dashed vertical lines (- - -) indicate the lower and upper limits of the relaxation times τ probed in the experiments.

where τ_0 is a constant, W is a constant related to activation energy of the relaxation process, and T_0 is the Vogel temperature related to the glass transition T_g of the material. For $T_0 = 0$, Eq. (5) reproduces Arrhenius' expression, $\tau = \tau_0 \exp[W(k_b T)^{-1}]$ with $k_b = 86.1321\ \mu e\mathrm{VK}^{-1}$. In Fig. 4, the relaxation map extracted from the DRT analyses at different temperatures is shown with gray scale. In order to compare both analyses, we plot the DRT and HNEF results with solid (——) and dashed (- - -) lines, respectively. Moreover, results from the literature [13, 14] are also given [chained line (- · -)]. The β relaxation is omitted, since it has a very broad distribution and a low magnitude compared to the α-relaxations as presented in Fig. 3c. The fit parameters for the VFT and Arrhenius expressions and the values from the literature are presented in Table 1. The α_a relaxation is known to be asymmetric, and our investigations by means of Lévy statistics confirm this observation—we are able to fit two symmetric relaxations that result in two different VFT expressions, see the

Table 1
Fitting parameters for the α relaxations. T_g is determined by the temperature at which the VFT fits yield $\log \tau = 2$.

	$\log(\tau_0$ [s])	W [eV]	T_0 [K]	T_g [K]	Note
		α_a relaxation			
This work	−13.6	0.079	191.0	223.4	DRT
This work	−12.8	0.085	191.3	224.0	DRT
This work	−13.1	0.076	195.6	225.4	HNEF
Bella et al. [13]	−13.1	0.088	187.5	222.1	HNEF
		α_c relaxation			
This work	−16.6	0.40	——	——	DRT
This work	−18.4	0.45	——	——	HNEF
Bella et al. [13]	−19.3	0.49	——	——	HNEF

solid lines (——) in Fig. 4. The α_a distribution is symmetric at low temperatures, but becomes asymmetric around 250 K. When the fitting results are taken into consideration, there are slight differences between our studies and those of Bella et al. [13] and Grimau et al. [14], which are probably due to differences in the preparation and the thermal history of the materials.

Here, we presented the results of dielectric-data analyses for α-phase PVDF with two different techniques. For our particular material, both techniques result in equivalent temperature dependencies, which were also compared to data in the literature. Our numerical method for finding the DRT yields unique distributions for given dielectric data without any *a-priori* assumption. We have thus demonstrated that the dielectric data of materials can be analyzed

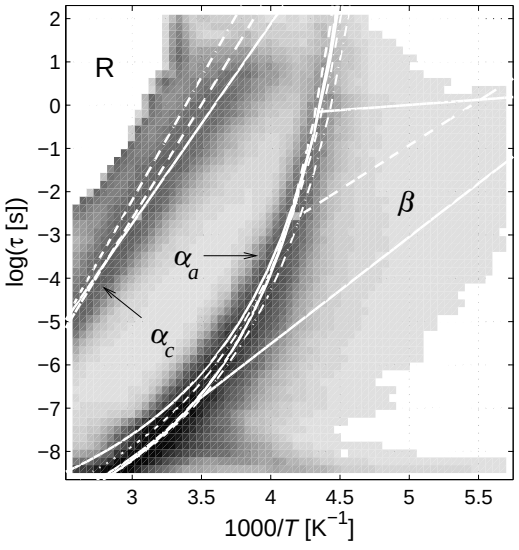

Fig. 4. Relaxation map for α-phase PVDF, which clearly shows the α_a and α_c modes. Solid (——) and dashed (- - -) lines represent the fits to VFT or Arrhenius expressions for the DRT and HNEF analyses, respectively. The results of Grimau et al. [14] and Bella et al. [13] are plotted as chained lines (- · -). The gray scale illustrates the probability density of the relaxations $\mathsf{g}(\tau)$, dark areas are the most probable regions for the particular relaxations. The omitted (white) region, labeled R, would contain molecular information related to melting of the sample.

with a more general representation than the empirical formulas. The DRT method might be useful to investigate the origin of dielectric relaxations and the electrical properties of materials.

References

[1] F. Kremer and A. Schönhals, eds., *Broadband Dielectric Spectroscopy* (Springer-Verlag, Berlin, 2003).

[2] A. K. Jonscher, *Dielectric Relaxation in Solids* (London: Chelsea Dielectric, London, 1983).

[3] J. R. Macdonald, J Comput Phys **157**, 280 (2000).

[4] J. R. Macdonald, ed., *Impedance Spectroscopy* (John Wiley & Sons, New York, 1987).

[5] E. Tuncer and S. M. Gubański, IEEE T Dielect El In **8**, 310 (2001).

[6] F. Riesz and B. Sz.-Nagy, *Functional Analysis* (Fredrick Ungar Publ. Co., New York, 1955), Dover ed.

[7] V. Volterra, Rend Accad Lincei **5**, 177 (1896).

[8] I. Fredholm, Kong. Vetenskaps-Akademiens Förh. Stockholm pp. 39–46 (1990).

[9] E. Tuncer, *Dielectric properties of composite structures and filled polymeric composite materials*, Licenciate thesis–Tech. rep. 338 L, Department of Electric Power Eng., Chalmers University of Technology, Gothenburg, Sweden (2000).

[10] E. Tuncer, *Extracting spectral density function of a binary composite without a-priori assumption* (2004), `arXiv:cond-mat/0403243`.

[11] E. Tuncer, M. Furlani, and B.-E. Mellander, J Appl Phys **95**(6), 3131 (2004).

[12] J. R. Macdonald, J Chem Phys **102**(15) (1995).

[13] A. Bella, E. Laredo, and M. Grimau, Phys Rev B **60**(18), 12764 (1999).

[14] M. Grimau, E. Laredo, A. Bello, and N. Suarez, J Polym Sci Pol Phys **35**, 2483 (1997).

[15] K. Tashiro, in *Ferroelectric Polymers: Chemistry, Physics and Applications*, edited by H. R. Nalwa (Marcel Dekker Inc., New York, 1995), chap. 2.

[16] B.-J. Jungnickel, in *Ferroelectric Polymers: Chemistry, Physics and Applications*, edited by H. R. Nalwa (Marcel Dekker Inc., New York, 1995), chap. 4.

[17] S. Havriliak and S. Negami, J Polym Sci Pol Lett **14**, 99 (1966).

[18] E. Tuncer, J Phys D Appl Phys **37**, 334 (2004), `arXiv:cond-mat/0403244`.

[19] M. Adlers, *Least Squares Problems with Box Constraints*, Licenciate thesis—Tech. rep. LiTH-MAT-R-1998-19, Department of Mathematics, Linköping University, Linköping, Sweden (1998).

[20] C. Lawson and R. Hanson, *Solving Least Squares Problems* (Prentice-Hall, Englewood Cliffs, NJ, 1974).
[21] L. Breiman, *Probability*, Addison-Wesley Series in Statistics (Addison-Wesley Publishing Company, Inc., Reading, 1968).
[22] W. Feller, *An Introduction to Probability Theory and Its Applications*, vol. 2 (John Wiley and Sons, New York, 1970).
[23] G. S. Fulcher, J Am Ceram Soc **8**, 339 (1925).
[24] G. Tammann and W. Hesse, Z Anorg Allg Chem **159**, 245 (1926).
[25] H. Vogel, Phys Z Leipzig **22**, 645 (1921).